Ab Initio Calculations of the Structure, Kinetics, and Infrared Laser Chemical Reaction Dynamics of Fluorooxirane†

Tae-Kyu Ha, Jörg Pochert, and Martin Quack*

Laboratorium für Physikalische Chemie, Swiss Federal Institute of Technology, ETH-Zürich (Zentrum), CH-8092 Zürich, Switzerland

Received: November 7, 1997; In Final Form: March 18, 1998

We report results of ab initio calculations on the main features of the potential energy hypersurface of fluorooxirane H_2COCHF near the equilibrium geometry and for several possible reaction pathways in thermal, chemical activation, and infrared laser chemical experiments. The ab initio results are compared to recent spectroscopic and kinetic data for this compound. The laser chemical reaction dynamics during and after infrared multiphoton excitation is simulated in detail ab initio and with adjustment of some of the potential parameters to reproduce the experimentally dominant channels leading to ketene and HF (or DF) for various isotopomers.

1. Introduction

Recently we reported the synthesis of fluorooxirane and derived its structure (see Figure 1) from high resolution infrared spectroscopic data.[1] Spectroscopic and kinetic data show that H_2COCHF and its doubly deuterated isotopomer D_2COCHF decompose during and after IR multiphoton excitation according to the following reaction scheme to give ketene and hydrogen fluoride.

$$D_2COCHF \xrightarrow{nh\nu} \begin{cases} \xrightarrow{\alpha\alpha} D_2C{=}C{=}O + HF & \text{(Ia)} \\ \xrightarrow{\alpha\beta} HDC{=}C{=}O + DF & \text{(Ib)} \end{cases}$$

Approximately $n = 24$ infrared photons of wavenumber $\tilde{\nu} = 1083$ cm^{-1}, absorbed by the C−F stretching chromophore vibration are necessary to reach the reaction threshold. A branching ratio between the two pathways of nearly two to one is observed, favoring the production of the doubly deuterated ketene and HF (reaction Ia). The different reaction products indicate that there are at least two distinct pathways for elimination. In general there are direct and complex eliminations, the latter passing through rearrangement to the metastable intermediates fluoroacetaldehyde or acetylfluoride, followed by elimination. Furthermore a laser chemical steady state rate coefficient of $k(\mathrm{st}) = 1.5 \times 10^7$ s^{-1} at a laser intensity of $I = 100$ MW cm^{-2} is obtained experimentally.

In the present paper we address the following questions: Is it possible to identify the reaction mechanism of the eliminations theoretically and to predict the observed IR laser chemical reaction dynamics without experimental information? How do calculated and experimental data compare? Is it possible to improve the theoretical results by adjusting some important quantities to experiment? The answers are of interest for understanding the unimolecular reaction dynamics of fluorooxirane, and they provide a test for the quality of ab initio calculations and the theoretical treatment of IR laser chemistry.

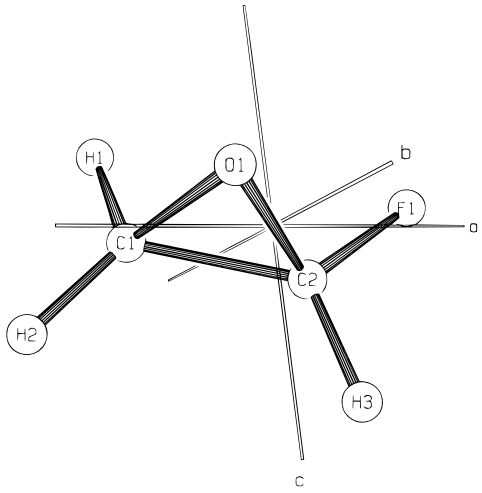

Figure 1. Structure of fluorooxirane calculated at the MP2(full)/TZ2P level of theory. Numerical data are listed in Table 1. The center of mass system of inertial axes (*abc*) is shown.

The first step to answer these questions is to calculate the properties of the potential energy hypersurface (PES) of fluorooxirane ab initio, including transition structures, reaction products, their relative energies, and harmonic vibrational frequencies. Because the IR multiphoton excitation is governed by processes on the electronic ground state of the reactant, it should be possible to obtain relatively accurate information about the basic parameters for the reaction dynamics from ab initio calculations. In a second step, the specific rate coefficients for the possible unimolecular reaction channels are calculated from the statistical theory of unimolecular reactions. In the third step, the infrared multiphoton excitation is simulated by a nonlinear case B/C master equation approach to obtain product yields and branching ratios as well as their dependence on laser and molecular parameters.

Beyond the reaction dynamics studied here, the PES of fluorooxirane is of importance for the chemical activation of

* Corresponding author: Laboratorium für Physikalische Chemie, ETH−Zürich (Zentrum), CH-8092 Zürich, Switzerland. Phone: +41/1/6324421. Fax:+41/1/6321021. E-mail: quack@ir.phys.chem.ethz.ch.

† Presented at the 10th International Congress of Quantum Chemistry, Atlanta, June 1997, and dedicated to Dieter Seebach on the occasion of his 60th birthday.

S1089-5639(98)00122-4 CCC: $15.00
Published on Web 06/17/1998

fluoroethylene with oxygen atoms (^{1}D or ^{3}P)[2]

$$O + H_2C{=}CHF \rightarrow CH_2OCHF \rightarrow \text{Products} \qquad \text{(II)}$$

which is of interest in atmospheric chemistry. The PES is also important for the racemization reaction of these optically active compounds including the context of parity violation,[3] as well as for chiral selection by multiphoton excitation.[4]

2. Theoretical Methods

2.1. Ab Initio Calculations. We performed ab initio molecular orbital calculations using the Gaussian 94,[5] Gamess,[6] and AcesII[7] program packages. Initial geometry optimizations were carried out at the unrestricted Hartree−Fock level of theory (UHF) with the 6-31G(d,p) basis set.[8] Saddle points of order 1 (transition structures) were located using the information of the hessian matrix either directly or with an eigenvalue following algorithm. The identity of each transition structure is established by an intrinsic reaction coordinate calculation at the same level of theory. Geometries were then reoptimized and harmonic vibrational frequencies were calculated with the second-order Møller−Plesset perturbation theory (MP2)[9] using the 6-311G-(d,p) basis set.[10] Improved energies of all stationary points were obtained via single-point electronic energy calculations at the MP2-optimized geometries with the quadratic configuration interaction method QCISD(T)[11] using the 6-311G(d,p) basis set and with the coupled cluster theory CCSD(T)[12] in conjunction with the 6-311G(d,p) and the TZP basis sets.[13] In the correlated calculations, all electrons, including the core, were treated. To check for biradical structures, an additional CASSCF complete active space calculation[14] with three configurations and the 6-31G(2d) basis set was carried out at each stationary point. The equilibrium properties of fluorooxirane were calculated furthermore with the larger TZ2P (C,F,O, (10s6p2d)/[5s4p2d]; H, (5s2p)/[3s2p]) basis set,[15] including harmonic vibrational frequencies and absolute infrared intensities G. To predict the reaction dynamics, the harmonic vibrational zero point energies of all deuterated and not deuterated species were calculated (MP2, 6-311G(d,p)) and added to the electronic energies (CCSD(T), TZP).

2.2. Thermal and Specific Rate Coefficients. The reaction dynamics is calculated by means of the mechanistic information obtained ab initio. Transition states are approximated by saddle points of order one on the PES, and reaction thresholds E_T are taken as differences between reactant and transition state energies including harmonic zero point corrections (usually for the example of the doubly deuterated species). The specific rate coefficients $k(E, J)$ can be calculated from statistical theories of unimolecular reactions:[16]

$$k(E, J) = \frac{W(E, J)}{h\rho(E, J)} \qquad (1)$$

$\rho(E, J)$ denotes the density of states of the reactant, $W(E, J)$ is the number of open adiabatic channels or quantum states of the transition state at energy E, and J is the angular momentum quantum number. In practice, we have neglected the angular momentum dependence in the present calculations (nominally for $J = 0$), which is similar to a semirigid transition state in a simple RRKM model. $\rho(E)$ and $W(E)$ are obtained from harmonic, vibrational frequencies calculated ab initio, applying a quantum mechanical counting algorithm.[17] Only for the pumped C−F stretching vibration anharmonicity corresponding to a Morse oscillator with effective dissociation wavenumber $D_e = 45000$ cm^{-1} is assumed. For the doubly deuterated fluorooxirane experimental vibrational fundamental frequencies[1] are used in our calculations with otherwise the same approximations. While some empirical anharmonicity corrections might be easily applied, and statistical adiabatic channel calculations would be feasible with greater effort, the errors resulting from the approximate treatment discussed are expected to be smaller than those arising from the uncertainties in the energies, calculated ab initio. Rate constants for the thermal reactions in the high pressure limit $k_\infty(T)$ can be obtained from transition state theory as

$$k_\infty(T) = \frac{kT}{h}\frac{Q^\dagger}{Q}\exp\left(-\frac{E_T}{RT}\right) \qquad (2)$$

where Q and $Q^\dagger$ are the complete partition functions of reactant and transition state. The thermal rate coefficients can be used to calculate the Arrhenius A-factors and activation energies E_A analyzing eq 2 with the Arrhenius formula:

$$k_\infty(T) = A_\infty(T)\exp\left(-\frac{E_{A,\infty}(T)}{RT}\right) \qquad (3)$$

2.3. Theory of IR Laser Chemistry. The calculation of the infrared multiphoton excitation and the laser chemical reaction dynamics was performed using the nonlinear case B/C master equation approach[18,19] of the form

$$\frac{d\mathbf{p}}{dt} = \mathbf{K}\mathbf{p} \qquad (4)$$

where $\mathbf{p}$ is the time dependent population vector of coarse grained molecular energy levels, spaced by one laser photon and $\mathbf{K}$ denotes the rate coefficient matrix. The rate coefficients for absorption $K_{M+1,M}$ are:[18]

$$K_{M+1,M} = \frac{\pi}{2}\langle|V_{M+1,M}|^2\rangle/\delta_{M+1} \qquad (5)$$

Here δ_{M+1} is the average angular frequency spacing in level $M + 1$, inversely proportional to the effective density of states ρ_{M+1} in this level. $\langle|V_{JI}|\rangle$ denotes the average coupling matrix element between two coarse grained levels, given by

$$|V_{JI}|^2 = \frac{1}{N_I}\frac{1}{N_J}\sum_{i=1}^{N_I}\sum_{j=1}^{N_J}|V_{j(J)i(I)}|^2 \qquad (6)$$

where

$$|V_{ji}| = -|M_{ji}||E_0|/\hbar \qquad (7)$$

The summation in eq 6 is restricted to states i in level I and states j in level J with numbers N_I and N_J as indicated, M_{ji} is the electric transition dipole moment, and $|E_0|$ is the electric field amplitude of the radiation. For a relatively small molecule like fluorooxirane at low laser intensities and excitation levels, case C applies[18] and the effective rate coefficients for stimulated emission are given by[20]

$$K^C_{M,M+1} = K_{M+1,M}\left(\frac{\rho_M}{\rho_{M+1}}\right)\left[\frac{\pi}{2}\sqrt{3}\left(\frac{\langle|V_{M+1,M}|\rangle}{\delta_{M+1}}\right)\right]^{-1} \qquad (8)$$

$|V_{M+1,M}|^2$ is proportional to the laser intensity and thus $K^C_{M,M+1} \propto \sqrt{I}$, resulting in a nonlinear intensity dependence. At higher laser intensities ($I >$ 100 MW cm^{-2}) and higher levels of excitation a transition to the intensity proportional case B

takes place, with the rate coefficient for stimulated emission being given by:[18]

$$K^{B}_{M,M+1} = K_{M+1,M}\left(\frac{\rho_M}{\rho_{M+1}}\right) \quad (9)$$

Within the chromophore model, these rate coefficients can be parametrized with experimentally accessible quantities:[21,22]

$$K_{M+1,M} = \frac{CGI\rho'_M}{\Delta\tilde{E}\rho_M} \quad (10)$$

Here, G is the integrated band strength of the chromophore vibration, defined as[23]

$$G = \int_{\text{band}}\sigma(\nu)\nu^{-1}\mathrm{d}\nu \simeq \frac{1}{\nu_0}\int_{\text{band}}\sigma(\nu)\mathrm{d}\nu \quad (11)$$

Where σ is the absorption cross section and ν_0 is the position of the band center. $\Delta\tilde{E}$ is an adjustable bandwidth parameter, typically related to the excitation wavenumber by $\Delta\tilde{E} \simeq \tilde{\nu}_{\text{exc}}/4$, and I is the laser intensity. ρ_M is the total rovibronic density of states in the level M, ρ'_M is the rovibronic density of states without the chromophore vibration, and C can be regarded as a constant to a good approximation in many cases.

The diagonal elements of the K-matrix contain the specific rate constants $k(E, J)$ for unimolecular decay of the reactant at the energy E_M of laser level M.

$$K_{MM} = -(K_{M+1,M} + K_{M-1,M}) - k(E_M, J) \quad (12)$$

For constant laser intensity, the solution of the master equation is given by

$$\mathbf{p}(t) = \exp(\mathbf{K}t)\,\mathbf{p}(t_0) \quad (13)$$

which is calculated in practice by diagonalization of the rate coefficient matrix $\mathbf{K}$ with eigenvalues λ_i.[19] For long times, only one eigenvalue, λ_1, which is closest to zero, is dominant for the time evolution corresponding to a steady state. Then, the decay of the remaining fraction of reactants F_R is characterized by one single rate constant $k(\text{st})$ or $k_I(\text{st})$[18-20]

$$\lim_{t\to\infty}\left[-\frac{\mathrm{d}\ln(F_R)}{\mathrm{d}t}\right] = \lim_{t\to\infty}k(t) = k(\text{st}) = -\lambda_1 \quad (14)$$

$$\text{or} \qquad k_I(\text{st}) = \frac{k(\text{st})}{I} \quad (15)$$

Beyond the influence of molecular parameters, IR laser chemistry is determined by laser parameters. The radiation from the IR laser used in our experiments[1] is characterized by intensity I and laser fluence F, defined as

$$F = \int_0^t I(t')\mathrm{d}t' \quad (16)$$

The simulations of IR multiphoton excitation are carried out using the case B/C master equation, with a digitized single mode laser pulse of 200 ns duration, shown in Figure 2. For a total laser fluence of $F = 12$ J cm^{-2}, for example, a maximum intensity of 238 MW cm^{-2} is obtained. The solution of the master equation is obtained in steps corresponding to the region of constant intensity of the model pulse in Figure 2 using eq 13 in each step and a starting population $p(t_0)$ equal to the final population of the previous step. For all reactions under consideration the integrated band strengths for the pumped C−F stretch vibration is set to the value of $G = 1.48$ pm^2, as measured for the [^{2}H$_2$]−fluorooxirane. The excitation wavenumber is $\tilde{\nu}_{\text{exc}} = 1083$ cm^{-1}, corresponding to the laser line 9R28 in the experiments.

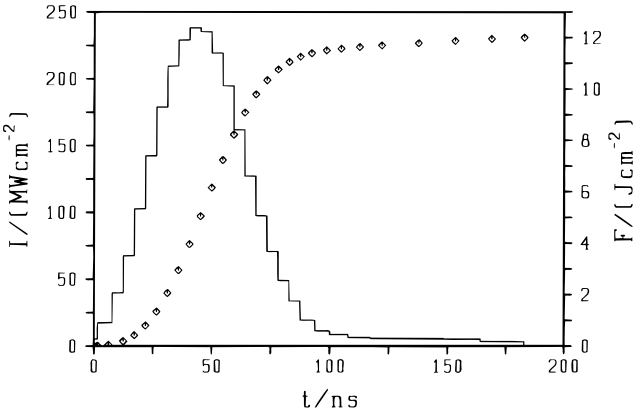

Figure 2. Model pulse for the calculation of infrared multiphoton excitation. The laser intensity (—) and fluence (diamonds) are given as a function of time. The total fluence is $F = 12$ J cm^{-2}.

TABLE 1: Full Optimized Structures of Fluorooxirane Calculated ab Initio at Different Levels of Theory[a]

coordinate	HF 6-31G(d,p)	MP2 6-311G(d,p)	MP2 TZ2P	ref 25	exp fit[1]
r(CC)	144.2	145.5	144.91	144.1	143.64
r(C^{1}O)	142.4	145.85	146.5	139.1	146.29
r(C^{2}O)	135.9	138.2	138.6		137.7
r(C^{2}H^1)	107.6	108.43	107.79	107.8	108.5
r(C^{1}H^2)	107.6	108.48	107.82	107.8	108.5
r(C^{1}H^3)	107.5	108.52	107.86	107.8	108.5
r(C^{2}F)	133.8	135.69	136.08	133.4	137.78
∠(C^{2}C^{1}O)	56.6	56.578	56.789		56.590
∠(C^{1}C^{2}H^1)	118.5	117.673	117.705		117.705
∠(C^{2}C^{1}H^2)	120.9	120.922	120.751		120.751
∠(C^{2}C^{1}H^3)	124.1	124.268	124.526		124.526
∠(C^{1}C^{2}F)	118.9	118.523	118.532		118.679
ϕ(H^1)	102.0	101.918	101.704		101.704
ϕ(H^2)	−101.5	−101.178	−101.192		−101.192
ϕ(H^3)	105.1	105.438	105.373		105.373
ϕ(F)	−104.9	−105.466	−105.442		−104.598

[a] Exp. fit refers to a partial r_0-structure taken from ref 1 which is fitted to reproduce the experimentally observed rotational constants. All bond lengths r are given in picometers pm, all bond angles ϕ and ∠ are given in degrees, and ϕ represents the dihedral angle of the atom in parentheses with the CCO plane. The numbers of the atoms are those of Figure 1.

Branching ratios for alternative reactions **a** and **b** can be derived by dividing the total product population integrated over time up to t_f in each level $p_N^{\text{tot},p}$ from both reactions into proportions according to

$$F_P^a = \sum_N p_N^{a,p}(t_f) = \sum_N \frac{k^a{}_N(E)}{k^a{}_N(E) + k^b{}_N(E)} p_N^{\text{tot},p}(t_f) \quad (17)$$

Here, $t_f = 200$ ns corresponds to a time after the end of the laser pulse.

3. Results

3.1. Equilibrium Properties of Fluorooxirane. The calculated structure of fluorooxirane is shown in Figure 1 and the corresponding numerical data are given in Table 1. Calculations

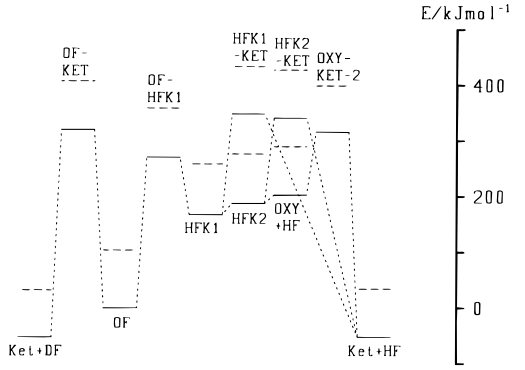

Figure 3. Direct eliminations of hydrogen fluoride from [$^2H_2$]−fluorooxirane (OF) to give ketene (KET). Energies are taken from Table 3. The solid lines represent the electronic energies, the dashed lines give electronic and zero point energies, and the dotted lines are used to indicate intrinsic reaction coordinate calculations. For explanation of acronyms see Figure 5 and Table 3.

of the equilibrium geometry have also been reported previously.[24,25] The compound shows a significant shortening of the HFC−O bond compared to the H_2C−O bond of about 8 pm indicating that the oxirane ring is rather strongly distorted. The values of the bond lengths and angles change by less than 1 pm or 1 degree on increasing the basis set from 6-311G(d,p) to TZ2P (Table 1) and the distortion of the CCO ring is increased only slightly. The harmonic vibrational frequencies of fluorooxirane and 2,2-[$^2H_2$]−fluorooxirane are calculated at several levels of theory and compared to experiment. Table 2 summarizes the results in comparison to experimental vibrational fundamental wavenumbers from ref 1. For the MP2(full)/TZ2P calculation of the frequencies, the deviation from experimental fundamentals is found to be in the range of 1−6%, in part due to anharmonicity. The band strengths G calculated in the double harmonic approximation are slightly larger than the experimental values, but the sequence of strongly and weakly absorbing bands is exactly the same in experiment and theory. In summary, the quality of the calculated infrared spectra is adequate for the description of fluorooxirane and its doubly deuterated isotopomer. At the SCF/TZ2P level of theory, a value of 2.7 D is obtained for the dipole moment, which is qualitatively consistent with the large pressure self-broadening coefficient of fluorooxirane which we measured to be 1.4 cm^{-1} bar^{-1} in the ν_9 band. The dipole moment components with respect to the inertial axes (Figure 1) are $|\mu_a| = 1.06$ D, $|\mu_b| = 2.02$ D, $|\mu_c| = 1.44$ D for H_2COCHF and $|\mu_a| = 1.19$ D, $|\mu_b| = 1.86$ D, $|\mu_c| = 1.55$ D for D_2COCHF.

3.2. Reaction Pathways. Because ketene and hydrogen fluoride and their deuterated isotopomers are the only reaction products observed experimentally (except for traces of carbon monoxide, see discussion below), we restrict our calculations largely to processes yielding these compounds. With the ab initio procedures described above 16 transition structures connecting nine different molecules were located on the PES. For the molecules we use acronyms. Transition structures are consequently named after the molecules which they connect as summarized in Table 3. We discuss three categories of reactions: Direct eliminations of HF or DF from fluorooxirane, complex eliminations passing via fluoroacetaldehyde or acetylfluoride as intermediates, and reactions leading to other products. Energy diagrams for the direct eliminations are shown in Figure 3, those for the complex eliminations are shown in Figure 4. Figure 5 summarizes the reaction pathways under consideration, and Figure 6 displays structures of the stationary points found. Energies are listed in Table 3.

TABLE 2: Harmonic Vibrational Frequencies ω, Absolute Band Strengths G, and Electronic Energies of Fluorooxirane and 2,2-[$^2H_2$]−Fluorooxirane Calculated ab Initio for Different Basis Sets and Methods Compared to Experimental Vibrational Fundamentals and Band Strengths, taken from Reference 1[a]

	C_2H_3FO												$[^2H_2]-C_2H_3FO$					
	HF/6-31G(d,p)		MP2(fc)/6-31G(d,p)		MP2(fc)/6-311G(d,p)		MP2/6-311G(d,p)		MP2/TZ2P				MP2/TZ2P					
					E_{el}/E_h						exp[1]		−252.681213		exp[1]			
	−251.731679		−252.313610		−252.477821		−252.553319		−252.681213									
no.	ω_{ai}/cm^{-1}	G_{ai}/pm^2	ω_{ai}/cm^{-1}	G_{ai}/pm^2	ω_{ai}/cm^{-1}	G_{ai}/pm^2	ω_{ai}/cm^{-1}	G_{ai}/pm^2	ω_{ai}/cm^{-1}	G_{ai}/pm^2	$\tilde{\nu}_{exp}$/cm^{-1}	G_{exp}/pm^2	ω_{ai}/cm^{-1}	G_{ai}/pm^2	$\tilde{\nu}_{exp}$/cm^{-1}	G_{exp}/pm^2
1	3390	0.11	3323	0.06	3276	0.06	3283	0.06	3289	0.02	3078		3235	0.07	3053	0.02
2	3361	0.12	3259	0.12	3221	0.11	3228	0.11	3235	0.06	3050	0.11	2457	0.02	2203	0.02
3	3290	0.07	3211	0.05	3166	0.05	3172	0.05	3176	0.04	3011		2304	0.03	2193	0.02
4	1684	0.53	1580	0.29	1553	0.36	1554	0.38	1541	0.27	1479	0.15	1444	0.96	1406	0.6
5	1571	0.67	1470	0.72	1448	0.70	1450	0.69	1427	0.66	1383	0.38	1328	0.25	1293	0.20
6	1439	0.27	1348	0.23	1338	0.27	1340	0.26	1319	0.33	1284	0.21	1189	0.07	1150	
7	1330	0.35	1215	0.14	1201	0.12	1203	0.12	1188	0.08	1156		1116	1.79	1101	1.48
8	1293	0.39	1190	0.74	1176	0.84	1178	0.87	1163	0.47	1135	1.14	1069	0.22	1044	
9	1271	1.07	1162	0.43	1158	0.52	1160	0.49	1148	0.90	1126		1000	0.59	982	0.259
10	1207	0.06	1121	0.04	1119	0.06	1121	0.06	1098	0.05	1058		875	0.28	867	0.147
11	1092	1.10	1003	0.83	998	0.90	1001	0.90	975	0.94	968	0.52	831	0.50	820	0.7
12	1014	0.88	913	1.15	904	1.21	907	1.19	881	1.39	867	0.71	816	0.49	803	
13	889	0.63	812	0.39	805	0.42	808	0.42	786	0.45	755	0.29	696	0.35	684	0.26
14	561	0.25	510	0.20	522	0.18	523	0.18	511	0.15	510	0.07	487	0.14	488	0.16
15	470	0.30	437	0.24	439	0.25	440	0.25	434	0.25	432	0.13	389	0.24	386	0.21

[a] fc indicates a "frozen core" calculation. Braces indicate the integration range for G in the case of integration over several bands.

TABLE 3: Reactions, Enthalpies (ΔH_0^0, ΔH_e^0), Threshold Energies (ΔE_0^T, ΔE_e^T) with (Index 0) and without (Index e) Zero Point Corrections, and Transition Structures (TS) Calculated ab Initio for Complex and Direct Eliminations from [$^2H_2$]−fluorooxirane To Give Ketene[a]

reaction	TS for react−prod	ΔH_e^0 (kJ mol^{-1})	ΔH_0^0 (kJ mol^{-1})	ΔE_e^T (kJ mol^{-1})	ΔE_0^T (kJ mol^{-1})
$D_2COCHF \xrightarrow{\alpha\beta} HDC{=}C{=}O + DF$	OF−KET	−52.3	−71.6	320.2	304.0
$D_2COCHF \xrightarrow{\alpha\alpha} D_2COC + HF$	OF−HFK1	167.5	155.2	270.7	255.3
$D_2COC + HF \rightarrow D_2C{=}C{=}O + HF$	HFK1−KET	−219.8	−224.5	181.3	174.9
$D_2COCHF \xrightarrow{\alpha\alpha} D_2COC + HF$	→HFK2	187.9	173.2		
$D_2COC + HF \rightarrow D_2C{=}C{=}O + HF$	HFK2−KET	−240.2	−242.5	153.2	150.6
$D_2COCHF \xrightarrow{\alpha\alpha} D_2COC + HF$	→OXY	202.8	186.0		
$D_2COC + HF \xrightarrow{\alpha\alpha} D_2C{=}C{=}O + HF$	OXY−KET-2	−255.1	−255.3	106.3	93.3
$D_2COC + HF \xrightarrow{\alpha\alpha} D_2C{=}C{=}O + HF$	OXY−KET	−255.1	−255.3	133.3*	118.8*
$D_2COCHF \rightarrow HD_2C{-}CFO$	OF−ACF	−179.4	−181.1	289.9*	275.2*
$HD_2C{-}CFO \xrightarrow{2,3} HDC{=}C{=}O + DF$	ACF−KET	133.8	109.5	260.9	246.9
$HD_2C{-}CFO \xrightarrow{2,3} D_2C{=}C{=}O + HF$	ACF−KET	133.8	111.8	260.9	244.9
$D_2COCHF \rightarrow HDFC{-}CDO$	OF−FAC-2	−72.7	−76.4	316.6	296.9
$HDFC{-}CDO \xrightarrow{3,3} D_2C{=}C{=}O + HF$	FAC−KET-2	20.4	7.1	350.9	333.0
$HDFC{-}CDO \xrightarrow{3,3} HDC{=}C{=}O + DF$	FAC−KET-2	20.4	4.8	350.9	334.7
$HDFC{-}CDO \xrightarrow{2,3} HDC{=}C{=}O + DF$	FAC−KET	20.4	4.8	341.7	325.7
$D_2COCHF \rightarrow D_2FC{-}CHO$	OF−FAC	−72.7	−76.4	246.0	237.3
$D_2FC{-}CHO \xrightarrow{3,3} HDC{=}C{=}O + DF$	FAC−KET-2	20.4	4.8	350.9	334.7
$D_2FC{-}CHO \xrightarrow{2,3} D_2C{=}C{=}O + HF$	FAC−KET	20.4	7.1	350.9	321.7
$H_2COCHF \rightarrow CH{-}O{-}CH_3F$	OF−ETH	201.7	202.5	342.6	336.0
$H_2FC{-}CHO \rightarrow CO + CH_3F$	FAC−DI	−27.0	−38.1	360.8	345.6
$H_2FC{-}CHO \rightarrow CO + HF + {}^1CH_2$	FAC−DI2	388.8	342.5	366.1	345.3
$H_2COCHF \rightarrow H_2O + FC{\equiv}CH$		142.9	97.6		
$H_2COCHF \rightarrow H_2O + HF + C_2$		602.8	551.9		
$H_2COCHF \rightarrow CHF + H_2CO$		336.8	314.0		
$H_2COCHF \rightarrow H_2C{=}CHF + {}^1O$	no TS	665.0	588.4	665.0	588.4
$H_2COCHF \rightarrow H_2C{=}CHF + {}^3O$	$^1O \times {}^3O$	378.9	302.3	439.0	430.8
$H_2COCHF \rightarrow CO + CH_3F$		−88.4	−97.9		
$H_2COCHF \rightarrow H_2C{=}C{=}O + HF$		−50.6	−69.4		

[a] Threshold energies are calculated with respect to the minimum (e) or zero point (0) level of the reactants given in the column reaction. Top. Energies: CCSD(T)/TZP single point, geometries, and harmonic zero point correction, UMP2/6-311G(d,p). The marked (*) values correspond to calculations with the 6-311G(d,p) basis set. With this basis set one obtains for the first two reactions: $\Delta E_0^T = 317.0$ kJ mol^{-1} (via OF−HFK1) and $\Delta E_0^T = 267.2$ kJ mol^{-1} (via OF−HFK1). Middle: Reactions of fluorooxirane not leading to ketene and hydrogen fluoride. Bottom: Further reaction enthalpies calculated completely at the UMP2/6-311G(d,p) level of theory. $^1O \times {}^3O$ is the transition structure, estimated from the crossing point for singlet and triplet surfaces, with zero point corrections calculated at the UHF/6-31G(d,p) level of theory.

For the direct reaction pathways, a concerted $\alpha\beta$ DF elimination from fluorooxirane (OF) passing via the transition structure OF−KET to the singly deuterated ketene is observed, if electron correlation is included in the electronic energy calculation (see section 2.1). Only at the UHF level of theory one finds a carbene-like intermediate, which rearranges over a small barrier to ketene. This is documented in the literature about the widely investigated PES of C_2H_2O, too.[26−29] For the direct $\alpha\alpha$ elimination, one finds at first dissociation of HF from the oxirane ring via the transition structure OF−HFK1, followed by ring opening to ketene as the rate determining step. Here, three possible reactive intermediates exist, differing only by the position of the HF with respect to the remaining doubly deuterated oxiranylidene (Figure 6): HFK1, where the HF is loosely bound to the free electron pair, HFK2 with an oxygen-bound HF and OXY, the free oxiranylidene. These intermedi-

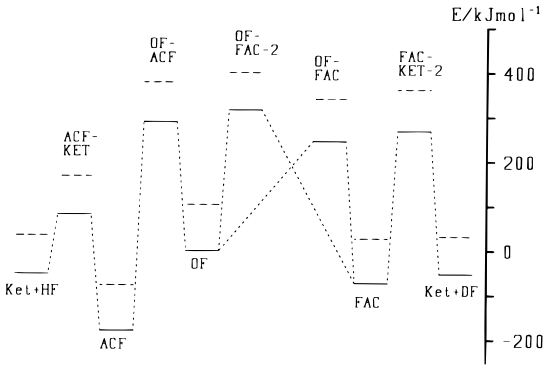

Figure 4. Complex pathways for the elimination of hydrogen fluoride from fluorooxirane (OF), passing via the stable intermediates acetylfluoride (ACF) and fluoroacetaldehyde (FAC) to ketene (KET). Energies are taken from Table 3. The solid lines represent the electronic energies, the dashed lines give electronic and zero point energies, and the dotted lines are used to indicate intrinsic reaction coordinate calculations. For explanation of acronyms, see Figure 5 and text.

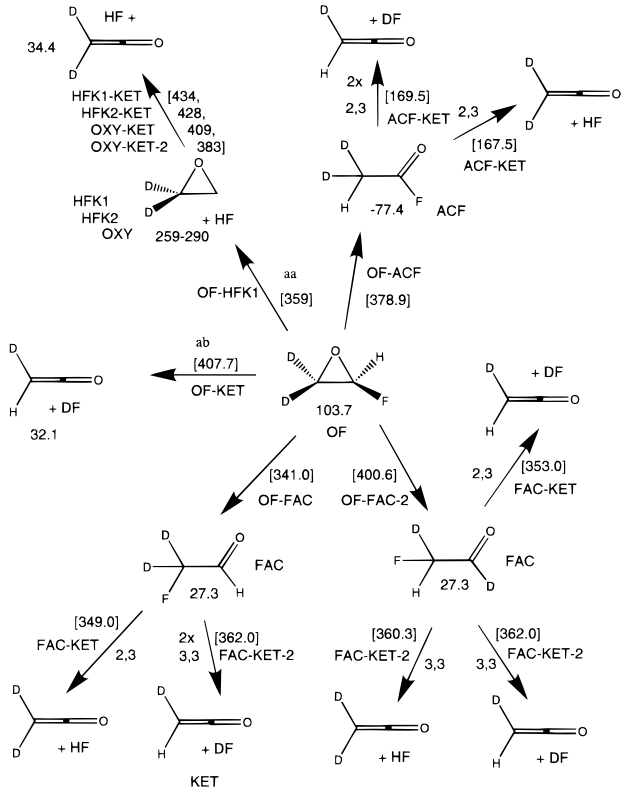

Figure 5. Elimination pathways of hydrogen and deuterium fluoride from 2,2-[$^2H_2$]−fluorooxirane (OF) calculated ab initio. The numbers given are energies (taken from Table 3) in kJ mol^{-1} including harmonic zero point correction relative to the electronic ground state minimum of fluorooxirane. The energies of transition structures are given in square brackets. Acronyms are listed beneath the structures. Exact structures are shown in Figure 6.

ates can undergo ring opening via three transition structures (HFK1−KET, HFK2−KET, and OXY−KET) with substantially higher barriers than the barrier of the dissociation step (OF−HFK1) to yield doubly deuterated ketene and HF. The minimum energy pathway for the ring opening of oxiranylidene and therefore for the completely direct αα elimination of HF does not correspond to one of these transition structures, but rather to a dissociation and recombination of the CO and $^1CH_2$ fragments on the PES of C_2H_2O mentioned above. One transition structure (OXY−KET-2) of lower energy has been found connecting oxiranylidene and CO + $^1CH_2$ on the singlet

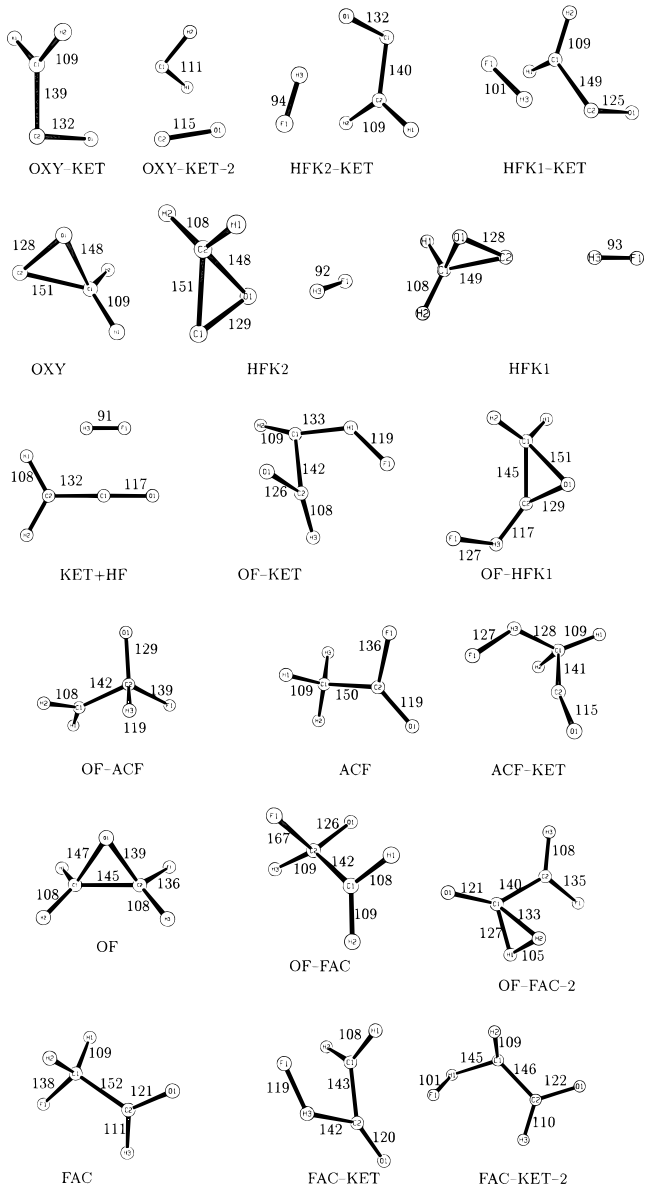

Figure 6. Structures of important stationary points for the PES of C_2H_3FO, calculated ab initio at the UMP2/6-311G(d,p) level of theory. See Table 2S (Supporting Information) for the coordinate values and Table 7 for vibrational frequencies. Bond lengths are given in picometers.

surface, where they can then recombine to ketene without barrier, as is illustrated by (*) in Figure 7. An incomplete recombination might furthermore be the reason for the observation of traces of carbon monoxide in the reaction mixture. The energy difference between the singlet (a^1A_1) and triplet (X^3B_1) carbene at the UMP2(full)/6-311G(d,p) level of theory is 75.5 kJ mol^{-1}, indicating, that an additional energy reduction might come from a spin forbidden process and that contributions of higher electronic states are important as well.[30] Recalculation of the PES of C_2H_2O at the CISD level of theory again yielded no barrier for the recombination of CO and carbene. The direct eliminations can be summarized by the following reactions:

$$D_2COCHF \rightarrow HDC{=}C{=}O + DF$$

$$\Delta E_{\text{eff}}^{\text{III}} = 304 \text{ kJ mol}^{-1} \quad \text{(III)}$$

$$D_2COCHF \rightleftharpoons D_2COC\cdots HF \rightarrow D_2C{=}C{=}O + HF$$

$$\Delta E_{\text{eff}}^{\text{IV}} = 279 \text{ kJ mol}^{-1} \quad \text{(IV)}$$

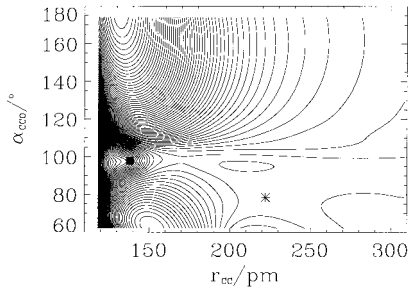

Figure 7. Two-dimensional relaxed PES of the $^1H_2C\cdots C{=}O$ combination and dissociation reaction in C_S symmetry. Points (340) have been calculated ab initio at the UMP2(full)/6-311G(d,p) level of theory. The carbon−carbon distance was varied between $R_{CC} = 118.4$ pm and 308.4 pm by 10 pm, the C−C−O angle was scanned from $\alpha_{CCO} = 62.12°$ by 7° to $\alpha_{CCO} = 174.12°$. Contour plot with energy difference $\Delta E = 2.61 \times 10^{-3}$ E_h between the lines. The coordinates of the transition structures OXY−KET-2 (star) and OXY−KET (square) are marked, the latter being difficult to identify visually in the figure as a transition structure.

The effective threshold energies ΔE_{eff} quoted here correspond to the thresholds that must be overcome along the reaction paths considered. They refer to the values of figure 5 minus the zero point energy of [$^2H_2$]−fluorooxirane (103.7 kJ mol^{-1}). For the complex reaction pathways, the elimination passes via rearrangement to the stable intermediates acetylfluoride (ACF) and fluoroacetaldehyde (FAC), which then undergo elimination of HF or DF to yield ketene (Figures 4 and 5). For the reaction via acetylfluoride, one transition structure has been found for the rearrangement (OF−ACF) and another (ACF−KET) for the 2,3 elimination of HF or DF, the latter being 2-fold degenerate. This is summarized in the following reactions:

$$D_2COCHF \rightarrow D_2HC{-}CFO \rightarrow D_2C{=}C{=}O + HF \qquad \Delta E_{eff}^{V} = 275 \text{ kJ mol}^{-1} \quad (V)$$

$$\rightarrow HDC{=}C{=}O + DF \qquad \Delta E_{eff}^{VI} = 275 \text{ kJ mol}^{-1} \quad (VI)$$

Fluoroacetaldehyde is produced either by passing via the transition structure OF−FAC to give $D_2FC{-}CHO$ or via OF−FAC-2, with an about 60 kJ mol^{-1} higher threshold, to give HDFC−CDO. Elimination occurs then as a 2,3 process via FAC−KET or as a 3,3 process via FAC−KET-2, where the DF abstraction from $D_2FC{-}CHO$ is again 2-fold degenerate. These eliminations are summarized as follows:

$$D_2COCHF \rightarrow D_2FC{-}CHO \rightarrow D_2C{=}C{=}O + HF \qquad \Delta E_{eff}^{VII} = 245 \text{ kJ mol}^{-1} \quad (VII)$$

$$\rightarrow HDC{=}C{=}O + DF \qquad \Delta E_{eff}^{VIII} = 258 \text{ kJ mol}^{-1} \quad (VIII)$$

$$D_2COCHF \rightarrow HDFC{-}CDO \rightarrow D_2C{=}C{=}O + HF \qquad \Delta E_{eff}^{IX} = 297 \text{ kJ mol}^{-1} \quad (IX)$$

$$\rightarrow HDC{=}C{=}O + DF \qquad \Delta E_{eff}^{X} = 297 \text{ kJ mol}^{-1} \quad (X)$$

Furthermore, there are reactions not leading to the observed products ketene and hydrogen fluoride. These include a rearrangement (via OF−ETH, $\Delta E_0^T = 336$ kJ mol^{-1}) of the fluorooxirane to the carbene-like ether (ETH), dissociation of fluoroacetaldehyde to the thermodynamically favored CO + CH_3F (via FAC−DI, $\Delta E_0^T = 345.6$ kJ mol^{-1}), or complete fragmentation to CO + $^1CH_2$ + HF (via FAC−DI-2, $\Delta E_0^T = 345.3$ kJ mol^{-1}), which have relatively low activation energies in the ab initio prediction. No low energy transition structure could be found, which would connect fluorooxirane and CO + CH_3F directly. In addition, the chemical activation of fluoroethylene with oxygen atoms was calculated. For this purpose relaxed PES scans of the singlet and triplet states were performed as a function of the rectangular O−CC distance. The effective barrier for the oxygen elimination is estimated from the energy of the crossing point ($^1O \times {}^3O$) between the singlet and triplet surface to be 430.8 kJ mol^{-1}, including zero point effects. However, this point shows one imaginary frequency at the UHF level and two, if correlation is included.

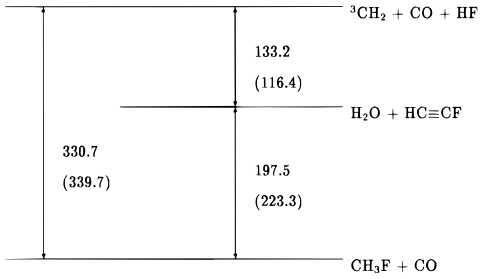

Figure 8. Differences of reaction enthalpies $\Delta\Delta H_0^0$ for reactions on the PES of C_2H_3FO. Values are calculated ab initio (UMP2/6-311G-(d,p)), and experimental data are given in parentheses.[31] Experimental uncertainties for $\Delta_f H_0^0$ are ±30 kJ mol^{-1} for CH_3F and ±60 kJ mol^{-1} for fluoroacetylene.

To estimate the quality of the ab initio results, calculated differences of reaction enthalpies $\Delta\Delta H_0^0$ including zero point corrections are compared to experimental data for similar reactions in Figure 8 (experimental data in parentheses taken from ref 31). Already at the UMP2/6-311G(d,p) level of theory the calculated values are within the rather large experimental error bars arising from the uncertainty of ±30 kJ mol^{-1} for $\Delta_f H_0^0$ of CH_3F and an uncertainty of ±60 kJ mol^{-1} for $\Delta_f H_0^0$ of fluoroacetylene. From experimental and ab initio data, the standard enthalpy of formation at 0 K of fluorooxirane is estimated to be $\Delta_f H_0^0 = (-229 \pm 30)$ kJ mol^{-1}.

For all structures a decrease in the ground state energy with increasing computational effort is observed (Table 1S, Supporting Information). Only for two stationary points (OXY−KET, OF−ACF) no convergence of the CCSD(T)/TZP calculation could be achieved. These points turned out to be biradicals, for which the single reference description is known to be inadequate. Additional single point CASSCF calculations were carried out to check the single reference results and to indicate the biradical nature of the corresponding stationary points. The results are given in Table 4. For biradicals more than one coefficient of the CI expansion differs appreciably from zero. This is the case for the transition structures OXY−KET and HFK2−KET of the direct ring opening reaction discussed above and for the rearrangements OF−ACF and OF−FAC for the complex eliminations. Therefore, the activation energies of these processes calculated from single reference methods might be wrong. On the other hand, MCSCF calculations are known to overestimate the biradical nature and projected and unprojected MP2 energies in the unrestricted calculations are the same for all stationary points ($\langle \hat{S}^2 \rangle = 0$), indicating the absence of spin contaminations.

In principle there is also interest in possible transition states for stereomutation of chiral fluorooxirane. While this is a problem of extra complexity several of the transition states for

TABLE 4: MCSCF/CASSCF Calculation with Two Excitations (Three Determinants) of Some Important Stationary Points of the C_2H_3FO−PES with the 6-31G(2d) Basis Set[a]

structure	E_{RHF}/E_h	E_{MCSCF}/E_h	$\|c_0\|^2$ [%]	$\|c_1\|^2$ [%]	$\|c_2\|^2$ [%]	$E_1 - E_0$ [kJ mol^{-1}]	$E_2 - E_0$ [kJ mol^{-1}]	Δ_{CI} [kJ mol^{-1}]
OXY−KET-2	−151.601 622	−151.628 739	99	0	1	1334.7	1983.1	71
OXY−KET	−151.551 642	−151.582 458	72	28	0	1557.3	2514.1	81
OF−FAC	−251.610 432	−251.646 040	50	41	9	738.9	1633.1	94
OF−FAC-2	−251.604 743	−251.622 149	98	1	1	3728.5	6517.1	46
HFK1−KET	−251.580 322	−251.610 037	94	0	4	1644.2	2659.1	78
HFK2−KET	−251.579 831	−251.610 273	64	31	5	830.0	1665.3	80
OF−ACF	−251.600 721	−251.656 537	23	65	12	711.6	1429.0	147
OF−HFK1	−251.592 816	−251.618 471	96	1	3	1585.9	2925.3	67
OF−KET	−251.575 977	−251.593 173	100	0	0	3727.3	6653.2	45
OF	−251.729 225	−251.745 156	100	0	0	2999.3	5200.7	42
KET	−151.731 109	−151.736 391	100	0	0	2352.6	4146.6	14
CH_2	−38.876 635	−38.878 756	100	0	0	32985.8	68435.6	6
CO	−112.744 421	−112.744 422	100	0	0	28896.2	59061.4	0

[a] Energies were calculated using the UHF/6-31G(d.p)-optimized structures. The listed coefficients c_i of the CI-expansion are those of the electronic ground state. The energy differences represent the excitation energy from the ground state to the first and second excited state of the same multiplicity ($S = 1$). The last column (Δ_{CI}) gives the difference in the electronic ground state energy $E_{RHF} - E_{MCSCF}$ between multiconfiguration and restricted Hartree−Fock calculations. For explanation of acronyms see Figure 5.

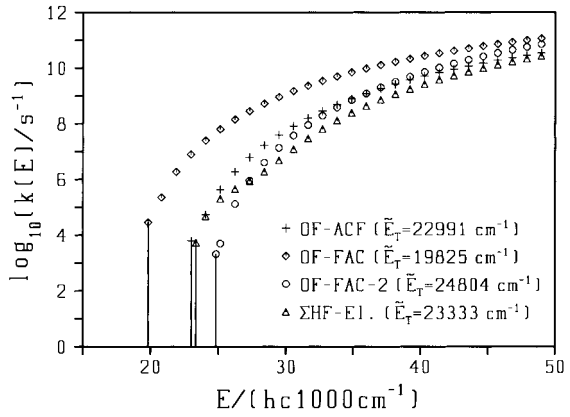

Figure 9. Logarithm of specific rate constants $k(E)$ as a function of energy for the unimolecular reactions of [$^2H_2$]−fluorooxirane: Rearrangement reactions to fluoroacetaldehyde (FAC, diamonds for OF−FAC, circles for OF−FAC-2), and acetylfluoride (ACF, crosses for OF−ACF). $\Sigma HF - El$ denotes the sum of the direct ($\sum\alpha\alpha$ as calculated from eq 18 and $\alpha\beta$, calculated from OF−KET) eliminations. OF−ACF, OF−FAC, and OF−FAC-2 denote the reactions to acetylfluoride and fluoroacetaldehyde via the corresponding transition states. Threshold wavenumbers $\tilde{E}_T$ (Table 3) are given in brackets and are indicated graphically by the solid lines. They refer to the zero point level of [$^2H_2$]−fluorooxirane.

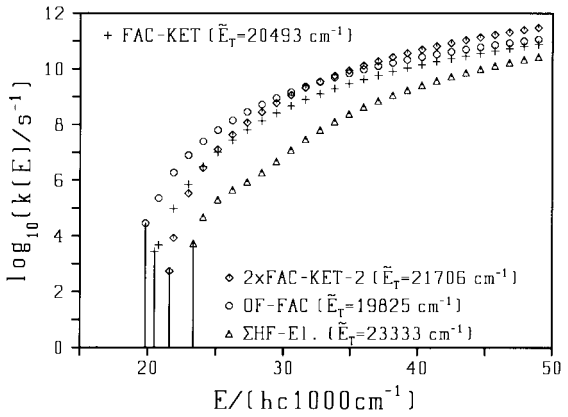

Figure 10. Logarithm of specific rate constants $k(E)$ as a function of energy for the direct eliminations from [$^2H_2$]−fluorooxirane to ketene compared to the complex eliminations from fluoroacetaldehyde (FAC) and acetylfluoride (ACF) at the same energy scale referring to the zero point level of [$^2H_2$]−fluorooxirane. $\Sigma HF - El$ denotes the sum of direct ($\sum\alpha\alpha$ as calculated from eq 18 and $\alpha\beta$, calculated from OF−KET) eliminations (triangles). FAC−KET (crosses) and (2×) FAC−KET-2 (diamonds) denote the reactions to ketene and fluoroacetaldehyde via the corresponding transition states. Threshold wavenumbers ($\tilde{E}_T$, indicated by solid lines, see Table 3) are given in parentheses. The values for the rearrangement of fluorooxirane to fluoroacetaldehyde (OF−FAC, circles) are given too.

elimination may be considered to provide upper bounds for racemization thresholds. A search for low energy transition states for stereomutation was not successful.

The effective threshold energies for all the investigated processes are within the range of 245−330 kJ mol^{-1}, which is a rather small bandwidth compared to the uncertainties. Therefore, several mechanisms are plausible for elimination.

3.3. Ab Initio Calculations of Laser Chemical Reaction Dynamics. The calculated minimum energy pathway from fluorooxirane to ketene and hydrogen fluoride corresponds to the rearrangement to fluoroacetaldehyde (via OF−FAC), followed by elimination of HF (via FAC−KET). The maximum energy threshold along this path is 245.3 kJ mol^{-1}. The specific rate coefficients (Figures 9 and 10) for the two reactions are calculated from the transition states mentioned. The observed branching ratio would here be a consequence of the alternative HF or DF eliminations from fluoroacetaldehyde. The reaction to HF (via FAC−KET) has a lower threshold energy (−13 kJ mol^{-1}) than the doubly degenerate DF elimination (via FAC−KET-2), but the specific rate coefficients show a crossing at energies of $\tilde{E} \simeq 24000$ cm^{-1} (Figure 10). The difference in threshold energies for rearrangement and (HF) elimination is only about 8 kJ mol^{-1}. Here, further assumptions are necessary to calculate the branching ratio. We therefore assume in one scenario that fluorooxirane is excited by the infrared laser to undergo a quick rearrangement to fluoroacetaldehyde followed by rate determining HF or DF elimination without appreciable collisional or radiative deactivation. The effective threshold energy for this process is assumed to be the energy difference between oxirane and the transition state FAC−KET (E_T = 20493 cm^{-1}) and HF and DF are produced with specific rate coefficients calculated from transition states FAC−KET and FAC−KET-2, respectively. The results are shown in Figure 11, the HF/DF ratio is calculated to be 1/1 compared to the observed value of 2/1 at a laser fluence of $F = 8$ J cm^{-2}, assuming a coupling width of $\Delta\tilde{E} = 160$ cm^{-1}. With the theoretical estimation of $\Delta\tilde{E} = \tilde{\nu}_{exc}/4 = 270$ cm^{-1} the calculated branching ratio is shifted towards the experimental value (2/1). Therefore one might conclude without knowing the experiment,

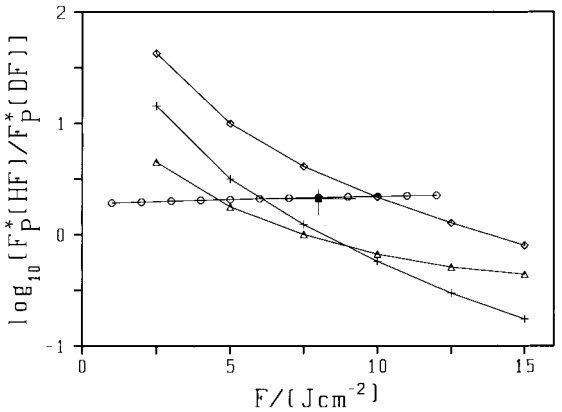

Figure 11. Logarithm of calculated HF/DF branching ratios for the direct and complex eliminations of HF or DF from [$^2H_2$]−fluorooxirane as a function of laser fluence for different reactions and coupling widths. The star indicates the summation in eq 17 over the combined product and reactant population above the threshold (i.e., product yields including after pulse dissociation[19]). The experimental value (square, $\tilde{\gamma}$ taken from ref 1) is shown for comparison. Triangles: $\Delta\tilde{E} = 160$ cm^{-1}, elimination from fluoroacetaldehyde Diamonds: $\Delta\tilde{E} = 270$ cm^{-1}, direct elimination from [$^2H_2$]−fluorooxirane. Crosses: As diamonds, but $\Delta\tilde{E} = 160$ cm^{-1}. Circles: Calculated from the laser chemical model with an empirical adjustment of threshold energies and with $\Delta\tilde{E} = 160$ cm^{-1}. See text for more detailed explanations.

that this channel might be important for the eliminations observed in ref 1. The laser chemical rate constant for the rearrangement step is calculated under the conditions listed in Table 5 to be $k_l(st) = 0.18$ cm^2 J^{-1}, comparable to $k_l(st) = 0.17$ cm^2 J^{-1} for the elimination step exciting fluoroacetaldehyde. Both values are compatible with the experimental value of $k_l(st) = 0.15$ cm^2 J^{-1} within the expected accuracy.

The next possible channel (with calculated threshold 30 kJ mol^{-1} higher) is the rearrangement to acetylfluoride via the biradical transition structure (OF−ACF). As already discussed, the threshold energy for processes with biradical intermediates might be reduced significantly due to contributions of higher excited electronic states. The specific rate coefficients are shown in Figure 9. They are comparable to those of the direct eliminations, discussed below. The HF/DF branching ratio for this mechanism is almost opposite to the observed one, because with similar threshold energies and frequency factors for HF and DF elimination (via ACF−KET) it is determined mainly by the reaction path degeneracy of almost two to one for the production of DF (Figure 5). The calculated laser chemical rate coefficients for rearrangement of fluorooxirane and elimination with acetylfluoride as reactant are $k_l(st) = 0.12$ and $k_l(st) = 0.4$ cm^2 J^{-1}, respectively, under the conditions listed in Table 5, indicating that the rearrangement would be the rate determining step here. Whereas the rate constants are compatible with experiment, the branching ratios are not. From this, one might exclude this mechanism.

Another 4 kJ mol^{-1} higher in threshold energy one finds the direct αα elimination of HF from fluorooxirane via the rate determining ring opening of oxiranylidene (via OXY−KET-2) to CO and $^1CH_2$ followed by recombination to ketene. The alternative DF production arises here from the direct αβ elimination (OF−KET). To evaluate the specific rate coefficients of the direct αα elimination, further assumptions are necessary because several processes are involved. At first, a fast microcanonical equilibrium between oxirane and oxiranylidene is assumed, passing over a modest barrier (OF−HFK) of 255 kJ mol^{-1}. This is plausible, because at an energy where significant amounts of ketene are produced the equilibration (10^7 s^{-1}) is 1 order of magnitude faster than the ring opening reaction of oxiranylidene (10^6 s^{-1}) or the αβ elimination. Secondly, there are three reactive intermediates (OXY, HFK1, HFK2) and interconversion between these structures is expected to be without substantial barrier. Therefore the ring opening is assumed to start from all three structures and the density of states of this complex reactant is calculated as a common reservoir of vibrational states:

$$k(E) = \sum_i k_i(E) = \sum_i \frac{W_i(E - E_{T,i})}{h\sum_k \rho_k(E - E_k)} \qquad (18)$$

W_i and $E_{T,i}$ are the number of quantum states and threshold energy of the ith transition state, and $\sum_k \rho_k(E - E_k)$ is the total common density of states of the complex reactant with E_k as the ground state energy of intermediate k. The $k(E)$ calculated from eq 18 are shown in Figure 12. The calculated HF/DF ratio for the direct eliminations from fluorooxirane is qualitatively in good agreement with experiment (diamonds and crosses in Figure 11). This agreement holds over a broad range of coupling widths, from (1.3/1) assuming $\Delta\tilde{E} = 160$ cm^{-1} to (3.9/1) taking $\Delta\tilde{E} = 270$ cm^{-1}, both for the fluence in the experiment

TABLE 5: Laser Chemical Steady State Rate Coefficients k_l(st) and k(st), Threshold Energies E_T, and Fraction of Product Molecules F_P for Several Reaction Channels with Transition State TS, Calculated ab Initio and Using the Case B/C master equation[d]

process	TS	E_T (kJ mol^{-1})	F_P	k_l (st) (cm^2 J^{-1})	k (st) (10^7 s^{-1})
$D_2COCHF \rightarrow D_2FC-CHO$	OF−FAC	237.3	0.54	0.18	1.8
$D_2FC-CHO \rightarrow D_2CCO + HF$	FAC−KET	325.7	0.47	0.17	1.7
$D_2COCHF \rightarrow D_2HC-CFO$	OF−ACF	275.2	0.37	0.12	1.2
$D_2HC-CFO \rightarrow D_2CCO + HF$	ACF−KET	244.9	0.87	0.40	4.0
$D_2COCHF \rightarrow HDCCO + DF$	OF−KET	304.0	0.26	0.08	0.8
$D_2COCHF{=}D_2COC\cdots HF$					
$D_2COC\cdots HF \rightarrow D_2CCO + HF$	HFK1−KET[a]	330.1	0.166	0.05	0.5
$D_2COCHF{=}D_2COC\cdots HF$					
$D_2COC\cdots HF \rightarrow D_2CCO + HF$	HFK1−KET[b]	304.0	0.26	0.08	0.8
$H_2COCHF \rightarrow H_2CCHF + {}^3O$	($^1O \times {}^3O$)[c]	430.8	8×10^{-4}	6×10^{-4}	6×10^{-3}
$D_2COCHF \rightarrow D_2CCO + HF$	Σαα	279.3	0.37	0.12	1.2
$D_2COCHF \rightarrow D_2CCO + HF$					
$D_2COCHF \rightarrow HDCCO + DF$	ΣHF	279.3	0.37	0.12	1.2

[a−c] See Table 6. [d] Laser parameters: Single mode pulse of 200 ns duration with maximum intensity of 238 MW cm^{-2} and a total fluence of $F = 12$ J cm^{-2}. Common molecular parameters: $G = 1.48$ pm^2, $\Delta\tilde{E} = 270$ cm^{-1}. The rate coefficients correspond to a laser fluence of 10.3 J cm^{-2} at an intensity of $I = 100$ MW cm^{-2}, where the steady state is reached. F_P corresponds to a time of 183 ns after the beginning of the pulse. Σαα denotes the direct αα elimination, with $k(E)$ calculated from eq 18 and E_T is the minimal threshold. ΣHF means the sum of direct (Σαα as calculated from eq 18 and αβ calculated from OF−KET) eliminations with E_T as minimal threshold.

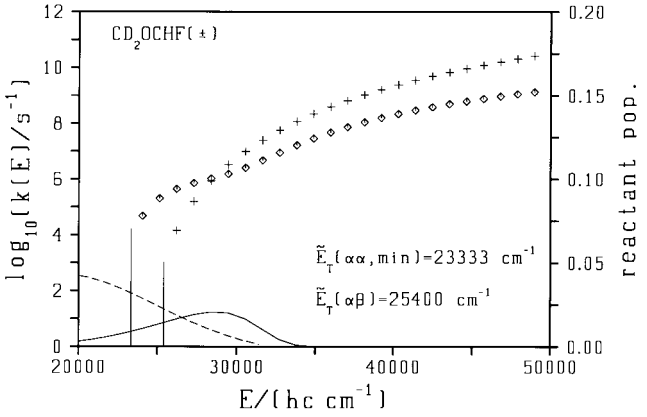

Figure 12. Logarithm of the specific rate constants $k(E)$ and population distributions over the reactant levels as a function of energy for the direct αα (as calculated from eq 18 and αβ (via OF−KET) eliminations of HF and DF from [$^2H_2$]−fluorooxirane. The population distributions over the reactant levels are shown after irradiation with single mode laser pulses of 200 ns duration (Figure 2) at laser fluences of $F = 5$ J cm^{-2} (− −) with $I_{max} = 99$ MW cm^{-2} and $F = 15$ J cm^{-2} (—) with $I_{max} = 297$ MW cm^{-2}. The coupling width is $\Delta E = 160$ cm^{-1}. The threshold wavenumbers $\tilde{E}_T$ (Table 3) are given for both channels.

($F = 8$ J cm^{-2}). The laser chemical rate constants under the conditions listed in Table 5 are $k_l(st) = 0.12$ cm^2 J^{-1} for the αα channel (HF) and $k_l(st) = 0.05$ cm^2 J^{-1} for the competing αβ elimination. This gives an overall value of $k_l(st) = 0.17$ cm^2 J^{-1} for the total reaction, which is in agreement with experiment.

Besides the IR laser driven decompositions, one might also look at the corresponding thermal reaction rates in the high pressure limit. Thermal rate coefficients calculated ab initio are listed in Table 6 for various processes. Because of the analogies between IR laser induced and thermal reactions, calculated thermal rate coefficients $k(T)$ mirror the general trends observed for the laser chemical coefficients $k_l(st)$, although especially branching ratios are expected to be different due to the different population distributions over reactant levels generated by the activation processes. Nevertheless, the rate determining steps in the consecutive reactions are the same here, for thermal and IR multiphoton activation.

The reaction dynamics calculated ab initio indicates that the direct eliminations or the reaction via fluoroacetaldehyde are the likely candidates for the overall mechanism. It is possible to reject the pathway via acetylfluoride. The rate constants and branching ratios calculated for the two more likely pathways are compatible with experiment, disregarding the ambiguity arising from the coupling width $\Delta\tilde{E}$, which can not be calculated exactly ab initio. The response of the branching ratio to the variation of $\Delta\tilde{E}$ as a parameter renders the direct eliminations to be the most likely reaction pathways. However, the threshold energies calculated ab initio would favor the reaction via fluoroacetaldehyde.

3.4. Adjustment to Experiment. We shall now use experimental information to reproduce the outcome of the experiments both qualitatively and quantitatively. We develop a simplified model for the IR laser chemistry of fluorooxirane and adjust potential parameters to the measured kinetic data. For the model description, the complex eliminations are ruled out for two reasons: Firstly, no traces of acetylfluoride or fluoroacetaldehyde have been observed in the reaction mixture even in experiments with collisional deactivation of intermediates by 20 mbar N_2, although these compounds should be detectable with high sensitivity by infrared spectroscopy. Secondly, as already pointed out, the direct eliminations calculated ab initio provide the better basis for the description of the measured data. Our model is shown in Figure 13.

Assuming again a fast equilibrium between oxirane and oxiranylidene via OF−HFK1 (section 3.3.), the rate determining steps of the two competing channels are represented by the transition states OF−KET for the DF and HFK1−KET for the HF elimination. The threshold energy for the αβ elimination corresponds to the value calculated ab initio ($\Delta E_{eff}^{III} = E_T^{\alpha\beta} =$ 304 kJ mol^{-1}, Table 3). For the competing αα elimination one might take first the calculated values too, to find

$$\Delta E_{eff}^{\alpha\alpha} = \Delta H_0^0(\mathrm{OF} \rightarrow \mathrm{HFK1}) + E_T^0(\mathrm{HFK1} \rightarrow \mathrm{KET} + \mathrm{HF}) = 330.1\ \mathrm{kJ\ mol^{-1}} \quad (19)$$

Alternatively, $\Delta E_{eff}^{\alpha\alpha}$ can be adjusted (Figure 13) to reproduce the observed branching ratio of 2/1 at a laser fluence of $F = 8$ J cm^{-1}. The reason to adjust the ring opening threshold is, that here additional uncertainties arise from possible singlet triplet conversion, biradical transition structures (OXY−KET), and the manifold of calculated reaction pathways. From this procedure, a value for the αα threshold energy of $\Delta E_{eff}^{\alpha\alpha} \simeq \Delta E_T^{\alpha\beta} \simeq 304$ kJ mol^{-1} is obtained. The branching ratio is therefore due to the

TABLE 6: Thermal High Pressure Rate Coefficients and Arrhenius Parameters for Some Unimolecular Reations on the C_2H_3FO−PES, Calculated ab Initio for Different Temperatures[d]

process	TS	T (K)	A (10^{13} s^{-1})	E_A (kJ mol^{-1})	k (T) (s^{-1})
$D_2COCHF \rightarrow D_2FC-CHO$	OF−FAC	500	4.9	241.3	3.1×10^{-2}
		1100	6.8	242.8	2.0×10^{2}
$D_2FC-CHO \rightarrow D_2CCO + HF$	FAC−KET	500	1.3	325.3	1.4×10^{-21}
		1100	4.6	332.1	8.0×10^{-3}
$D_2COCHF \rightarrow D_2HC-CFO$	OF−ACF	500	3.7	278.8	2.9×10^{-16}
		1100	6.3	281.6	2.7
$D_2HC-CFO \rightarrow D_2CCO + HF$	ACF−KET	500	3.6	248.8	3.9×10^{-13}
		1100	9.2	253.6	84.3
$D_2COCHF \rightarrow HDCCO + DF$	OF−KET	500	6.3	308.6	3.8×10^{-19}
		1100	14.7	312.9	0.21
$D_2COCHF{=}D_2COC\cdots HF$	HFK1−KET[a]	500	18.5	336.0	1.5×10^{-21}
$D_2COC\cdots HF \rightarrow D_2CCO + HF$		1100	44.7	340.5	0.031
$D_2COCHF{=}D_2COC\cdots HF$	HFK1−KET[b]	500	18.5	310	8.1×10^{-19}
$D_2COC\cdots HF \rightarrow D_2CCO + HF$		1100	44.7	314.4	0.54
$H_2COCHF \rightarrow H_2CCHF + {}^3O$	($^1O \times {}^3O$)[c]	500	11.1	434.9	4.4×10^{-32}
		1100	13.9	435.8	2.9×10^{-7}

[a] The effective αα threshold energy is $\Delta E_{eff}^{\alpha\alpha} = 330.1$ kJ mol^{-1}. [b] The effective αα threshold energy is adjusted to experiment ($\Delta E_{eff}^{\alpha\alpha} = 304$ kJ mol^{-1}). [c] The transition state is estimated from the crossing point of singlet and triplet surfaces. The column TS lists the corresponding transition states. [d] Energies are taken from Table 3.

TABLE 7: Harmonic Vibrational Frequencies of the Doubly Deuterated Compounds and Transition Structures (with One Imaginary Frequency $i = \sqrt{-1}$) on the $C_2H_2FO-PES^n$

FAC[a]	FAC[b]	ACF	HFK1[c]	HFK2[d]	OF−FAC	OF−FAC-2	ACF−KET[e]	OF−HFK-1	HFK1−KET	HFK2−KET	ACF−KET[f]	OF−KET
61	57	113	58	26	941*i*	986*i*	1238*i*	1350*i*	831*i*	1474*i*	1637*i*	1067*i*
312	305	388	76	36	266	188	248	230	232	124	224	283
526	528	505	161	129	440	341	313	276	268	147	309	360
606	596	597	619	365	535	433	423	592	385	261	400	548
936	931	839	637	381	586	592	551	747	527	432	565	677
963	970	893	724	689	784	777	628	816	640	667	617	703
1021	1005	940	752	732	887	786	805	844	824	784	773	834
1063	1099	1059	814	839	1021	908	913	906	906	882	888	914
1141	1172	1247	868	873	1123	1112	1031	1016	998	889	939	1008
1209	1319	1320	1037	1005	1308	1189	1096	1083	1122	946	1141	1070
1409	1383	1330	1101	1091	1409	1288	1302	1192	1244	1219	1323	1323
1795	1780	1921	1549	1489	1476	1394	1422	1480	1591	1359	1954	1376
2260	2209	2279	2317	2315	2307	1597	2191	2319	2297	2300	2193	1596
2359	2308	2368	2486	2484	2490	1873	2363	2487	2419	2449	2305	2386
2989	3145	3215	3922	4206	3133	3254	3213	2549	2470	3713	2423	3300

FAC−KET[f]	FAC−KET[g]	FAC−KET-2[h]	FAC−KET-2[i]	FAC−KET-2[j]	OXY[k]	KET[l]	KET[m]	OXY−KET-2	OXY-KET	OF−ACF	$^1O \times {}^3O$
2401*i*	1846*i*	561*i*	676*i*	555*i*	689	402	375	216*i*	2137*i*	1831*i*	584*i*
296	282	148	148	160	721	458	399	141	377	327	254
368	357	176	174	181	832	575	568	248	679	464	405
443	467	356	356	356	873	881	864	502	894	535	531
510	497	465	447	428	1003	1117	932	645	926	735	868
602	614	538	578	533	1092	1316	1245	1034	1264	772	1037
710	723	781	836	709	1507	2230	2212	2027	1345	881	1062
725	835	930	897	828	2313	2432	2379	2189	2287	948	1088
914	913	976	927	1040	2481	3303	2500	2305	2434	1077	1320
1069	1014	1099	951	1095						1203	1419
1122	1209	1199	1193	1403						1326	1563
1640	1293	1685	1686	1700						1389	1766
1880	1881	1906	2233	1906						2231	3370
2311	2383	2233	2355	2355						2295	3447
2464	3251	3201	2596	3023						2471	3482

[a] $D_2FC-HCO$. [b] HDFC−CDO. [c] $D_2COC{\cdot}HF$. [d] $D_2CCO{\cdot}HF$ [e] DF-elimination. [f] HF-elimination [g] DF-elimination. [h] HDFC−CDO → DF [i] HDFC−CDO → HF. [j] $D_2FC-CHO$ → DF. [k] D_2COC. [l] HDCCO. [m] D_2COO. $^1O \times {}^3O$: crossing point of singlet and triplet surfaces. [n] Values are calculated at the UMP2/6-311G(d,p) level of theory and given in cm^{-1}. Exception: $^1O \times {}^3O$, calculated at UHF/6-31G(d,p) level of theory.

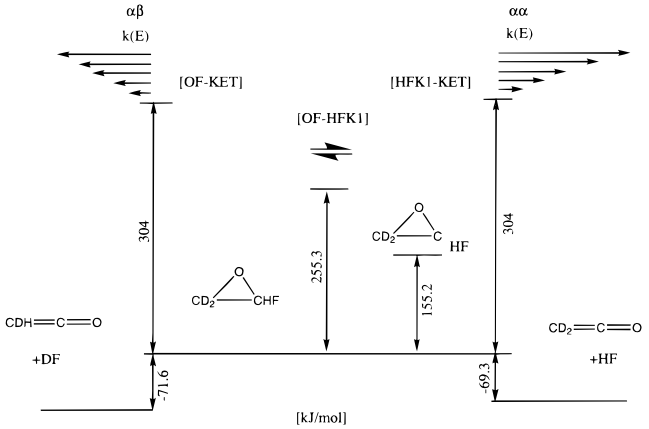

Figure 13. Simplified semiempirical model for the IR laser chemistry of [$^2H_2$]−fluorooxirane (OF). The whole process is represented by the direct eliminations (see text). The threshold energy for the DF elimination ($\alpha\beta$, via OF−KET) corresponds to the calculated value (Table 3). The ($\alpha\alpha$, via HFK1−KET) ring opening threshold to give doubly deuterated ketene and HF is adjusted to reproduce the experimental HF/DF branching ratio of 2/1. A preequilibrium (via OF−HFK1) for the production of the hydrogen fluoride complex 1 (HFK1, Figure 6) is assumed. The other energies correspond to those of Table 3 in kJ (mol^{-1}).

different "frequency factors" from the transition state frequencies leading to different Arrhenius A-factors in the case of thermal activation (Table 6).

Then, the coupling width $\Delta\tilde{E}$ can be obtained by fitting the simulated to the observed overall static reaction yield as a function of laser fluence.[1] This procedure circumvents some of the ambiguity arising from the coupling width. The static yield can be calculated from the convolution of the product fraction F_P calculated from eq 4 with the Gaussian spatial beam profile in the reaction cell. Here one finds a value of $\Delta E = 160\ cm^{-1}$. With these data, a value for the steady state rate constant of $k_I(st) = 0.28\ cm^2\ J^{-1}$ was derived from the simulation. This value can be compared to the experimental value of $k_I(st) = 0.15\ cm^2\ J^{-1}$, which is uncertain by about a factor of 2.[1] The calculated HF/DF branching ratio is only weakly dependent on laser fluence, as shown in Figure 11 (circles), consistent with experimental observations. Furthermore, the transition from the nonlinear case C to the linear case B of the theory of multiphoton excitation[19] is calculated to occur at a laser intensity of almost I=100 MW cm^{-2} for fluorooxirane.

4. Discussion and Conclusions

The stereochemical reaction dynamics of chiral molecules is usually investigated in the framework of the synthesis of relatively complex organic, possibly biologically important molecules including fluorinated species.[32,33] Indeed, only relatively few very small, rigid, and compact chiral molecules have been studied in detail with respect to their primary unimolecular reaction pathways. The recently synthesized fluorooxirane[1] is quite an outstanding example. Whereas already the experimental infrared laser chemistry of the isotopomer D_2COCHF points to several competing reaction channels,[1] our ab initio exploration of the potential energy hypersurface for this reaction system shows that there is a rich variety of close lying, possibly competing reaction channels as sum-

marized in Figure 5. Many of the transition structures shown in Figure 6 are highly nonrigid, stereochemically interesting species.

In the present paper we have first carried through a complete ab initio calculation of the infrared laser chemistry of fluorooxirane and in particular its [$^2H_2$]−isotopomer, starting out with spectroscopic properties, transition states, reaction enthalpies, and threshold energies. These data, derived from established ab initio approaches[5−15] are then combined with the theory of infrared multiphoton excitation and laser chemical reaction dynamics.[18−23] The end results of this complete ab initio calculation of laser chemical reaction dynamics, rarely carried through in such completeness so far for organic molecules, for the first time for a chiral molecule, to our knowledge, are the absolute laser chemical rate coefficients k_l(st) and the predicted relative branching ratios for various reaction channels. It turns out that the ab initio prediction for the latter is not in good agreement with experimental observations. The origin of the discrepancy can be easily understood by the great sensitivity of the predictions on the thresholds for various reaction channels, which fall all within the range of about seven infrared laser photons. The reliability of the calculated threshold energies to that degree is questionable because of the complex electronic structure of many of the transition structures and reaction intermediates. Whereas ab initio theory at the present level favours initial isomerization of fluorooxirane to fluoroacetaldehyde and subsequent HF (or DF) elimination, experimental observation clearly favors the direct, competing elimination pathways via OF−KET and HFK1−KET shown in Figure 5.

Relatively minor adjustments of the energy thresholds allow us to develop a semiempirical laser chemical reaction model, which is consistent with experimental observations. The adjustments (26 kJ mol^{-1}) are well within the uncertainties of current ab initio calculations. Some of the adjustments of the energy thresholds may also effectively represent the necessary multidimensional anharmonic corrections to the zero point energies and frequency factors, which may be very substantial for systems with very nonrigid transition structures, as has been demonstrated using advanced quasiadiabatic channel quantum Monte Carlo techniques.[34] These would require a complete 15-dimensional potential energy hypersurface for fluorooxirane, which is currently out of reach. Thus, in the present case we have to be satisfied with a simpler approach. Not surprisingly for a molecule which has just barely become accessible to experimental investigation, the present ab initio study has largely exploratory character. Future work may be directed towards more accurate descriptions of transition state energies, say, by MRCI methods, and to such questions as the influence of liquid solvents on transition state energies and reaction dynamics, which may be important for explaining some of the observations of stabilized intermediates in the low temperature chemical activation experiments.[2]

From the experimental side, the enantioselective synthesis of fluorooxirane with substantial enantiomeric excess remains a challenge, which would open up the possibility of studying laser chemical racemization dynamics,[3] the theoretical investigation of which is a theme by itself, hardly addressed in the present work on fluorooxirane.

We enjoyed help from and discussions with D. Luckhaus, H. F. Schaefer, III, G. Seyfang, and J. Stohner. Our work is supported financially by the Schweizerischer Nationalfonds and the ETH Zürich.

Supporting Information Available: Electronic energies and Cartesian coordinates of C_2H_3FO−PES (5 pages). Ordering information is given on any current masthead page.

References and Notes

(1) Hollenstein, H.; Luckhaus, D.; Pochert, J.; Quack, M.; Seyfang, G. *Angew. Chem., Int. Ed. Engl.* **1997**, *36*, 140.

(2) Menz, K. Untersuchung von Elementarreaktionen des atomaren Sauerstoffs in flüssigem Argon, Dissertation, Göttingen **1996**. Hack, W.; Menz, K. Private communication.

(3) Quack, M. *Angew. Chem., Int. Ed. Engl.* **1989**, *28*, 571.

(4) Pochert, J.; Quack, M.; Seyfang, G. To be published.

(5) Frisch, M. J.; Trucks, G. W.; Schlegel, H. B.; Gill, P. M. W.; Johnson, B. G.; Robb, M. A.; Cheeseman, J. R.; Keith, T.; Petersson, G. A.; Montgomery, J. A.; Raghavachari, K.; Al-Laham, M. A.; Zakrzewski, V. G.; Ortiz, J. V.; Foresman, J. B.; Cioslowski, J.; Stefanov, B. B.; Nanayakkara, A.; Challacombe, M.; Peng, C. Y.; Ayala, P. Y.; Chen, W.; Wong, M. W.; Andres, J. L.; Replogle, E. S.; Gomperts, R.; Martin, R. L.; Fox, D. J.; Binkley, J. S.; Defrees, D. J.; Baker, J.; Stewart, J. P.; Head-Gordon, M.; Gonzalez, C.; Pople, J. A. *Gaussian*; Gaussian, Inc.: Pittsburgh, PA, 1995.

(6) Schmidt, M. W.; Baldridge, K. K.; Boatz, J. A.; Elbert, S. T.; Gordon, M. S.; Jensen, J. H.; Koseki, K.; Matsunaga, N.; Nguyen, K. A.; Su, S. J.; Windus, T. L.; Dupuis, M.; Montgomery, J. A. *J. Comput. Chem.* **1993**, *14*, 1347.

(7) Shanton, J. F.; Gauss, J.; Watts, J. D.; Lauderdale, W. J.; Bartlett, R. J. ACESII, Version 1.0; 1992.

(8) Harriharam, P. C.; Pople, J. A. *Theor. Chim. Acta* **1972**, *28*, 212.

(9) Møller, C.; Plesset, M. S. *Phys. Rev.* **1934**, *46*, 618.

(10) Krishnan, R.; Binkley, J. S.; Seeger, R.; Pople, J. A. *J. Chem. Phys.* **1980**, *72*, 650.

(11) Bartlett, R. J.; Watts, J. D.; Kucharski, S. A.; Noga, J. *Chem. Phys. Lett.* **1990**, *165*, 513.

(12) Pople, J. A.; Head-Gordon, M.; Raghavachari, K. *J. Chem. Phys.* **1987**, *87*, 5968.

(13) Redman, L. T.; Purvis, D. D., III; Bartlett, R. J. *J. Am. Chem. Soc.* **1979**, *101*, 2856.

(14) Frisch, M. J.; Ragazos, I. N.; Robb, M. A.; Schlegel, H. B. *Chem. Phys. Lett.* **1992**, *189*, 524.

(15) Dunning, T. H. *J. Chem. Phys.* **1971**, *55*, 716.

(16) Quack, M.; Troe, J. In *Theoretical chemistry: advances and perspectives. (Theory of scattering, papers in honor of Henry Eyring)*; Henderson, D., Ed.; New York, Academic Press: New York, 1981; Vol. 6B, p 199; In *Enzyclopedia of Computational Chemistry*; von Ragué Schleyer, P., Allinger, N., Clark, T., Gasteiger, J., Kollman, P. A., Schaefer, H. F. Eds.; Wiley: New York, 1998. In press.

(17) Beyer, T.; Swinehart, D. F. *Commun. ACM* **1973**, *16*, 379.

(18) Quack, M. *J. Chem. Phys.* **1978**, *69*, 1282.

(19) Quack, M. *Adv. Chem. Phys.* **1982**, *50*, 395.

(20) Quack, M. *Ber. Bunsen-Ges. Phys. Chem.* **1981**, *85*, 318.

(21) Quack, M.; Schwarz, R.; Seyfang, G. *J. Chem. Phys.* **1992**, *96*, 8727.

(22) Lupo, D. W.; Quack, M. *Chem. Rev.* **1987**, *87*, 181.

(23) Quack, M. *J. Mol. Struct.* **1995**, *347*, 245.

(24) Furman, E. G.; Meleshevich, A. P. *Theor. Exp. Chem.* **1977**, *13*, 246.

(25) Saebo, S.; Almlöf, J.; Boggs, J. E.; Stark, J. G. *J. Mol. Struct.* **1989**, 200, 361.

(26) Bouma, W. J.; Nobes, R. H.; Radom, L.; Woodward, C. E. *J. Org. Chem.* **1982**, *47*, 1869.

(27) Tanaka, K.; Yoshimine, M. *J. Am. Chem. Soc.* **1980**, *102*, 7655.

(28) Vacek, G.; Galbraith, J. M.; Yamaguchi, Y.; Schaefer, H. F., III; Nobes, R. H.; Scott, A. P.; Radom, L. *J. Phys. Chem.* **1994**, *98*, 8660.

(29) Scott, A. P.; Nobes, R. H.; Schaefer, H. F., III; Radom, L. *J. Am. Chem. Soc.* **1994**, *116*, 10159.

(30) Schaefer, H. F., III *Science* **1986**, *231*, 1100.

(31) Chase, M. W.; Davies, C. A.; Downey, J. R.; Frurip, D. J.; McDonald, R. A.; Syverud, A. N. *J. Phys. Chem. Ref. Data* **1985**, 14.

(32) Blank, S.; Seebach, D. *Angew. Chem., Int. Ed. Eng.* **1993**, *32*, 1765.

(33) Gautschi, M.; Seebach, D. *Angew. Chem., Int. Ed. Eng.* **1992**, *31*, 1083.

(34) Quack, M.; Suhm, M. *Chem. Phys. Lett.* **1991**, *183*, 187.